



Carbon monoxide releasing molecule-3 alleviates neuron death after spinal cord injury *via* inflammasome regulation

Gang Zheng^{a,b,1}, Yu Zhan^{c,1}, Haoli Wang^{a,b,1}, Zucheng Luo^{a,b}, Fanghong Zheng^d, Yifei Zhou^{a,b,d}, Yaosen Wu^{a,b,d}, Sheng Wang^{a,b,d}, Yan Wu^e, Guangheng Xiang^{a,b}, Cong Xu^{a,b}, Huazi Xu^{a,b,d,*}, Naifeng Tian^{a,b,d,*}, Xiaolei Zhang^{a,b,d,f,*}

^a Department of Orthopaedics, The Second Affiliated Hospital and Yuying Children's Hospital of Wenzhou Medical University, Wenzhou 325000, Zhejiang Province, China

^b Zhejiang Provincial Key Laboratory of Orthopaedics, Wenzhou 325000, Zhejiang Province, China

^c Department of Chemoradiation Oncology, The First Affiliated Hospital of Wenzhou Medical University, Wenzhou 325000, Zhejiang Province, China

^d The Second School of Medicine, Wenzhou Medical University, Wenzhou 325000, Zhejiang Province, China

^e Department of Orthopaedics, The Second Affiliated Hospital, School of Medicine, Zhejiang University, 310058 Zhejiang Province, China

^f Chinese Orthopaedic Regenerative Medicine Society, Hangzhou 310058, Zhejiang Province, China

ARTICLE INFO

Article history:

Received 2 December 2018

Received in revised form 29 December 2018

Accepted 29 December 2018

Available online 3 January 2019

Keywords:

Spinal cord injury

Neuron death

Inflammasome

Carbon monoxide

ABSTRACT

Background: Genetic overexpression or pharmacological activation of heme oxygenase (HO) are identified as potential therapeutic target for spinal cord injury (SCI); however, the role of carbon monoxide (CO), which is a major product of haem degenerated by HO, in SCI remains unknown. Applying heme or chemicals which may regulate HO expression or activity to increase CO production are inadequate to elaborate the direct role of CO. Here, we assessed the effect of CO releasing molecule-3 (CORM-3), the classical donor of CO, in SCI and explained its possible protective mechanism.

Methods: Rat SCI model was performed with a vascular clip (30 g) compressing at T9 vertebral level for 1 min and CO was delivered immediately after SCI by CORM-3. The neurological deficits and neuron survival were assessed. Inflammasome and inositol-requiring enzyme 1 (IRE1) pathway were measured by western blot and immunofluorescence. For *in vitro* study, oxygen glucose deprivation (OGD) simulated the SCI-inflammasome change in cultured the primary neurons.

Findings: CORM-3 suppressed inflammasome signaling and pyroptosis occurrence, which consequently alleviated neuron death and improved motor functional recovery following SCI. As a pivotal sensor involving in endoplasmic reticulum stress-mediated inflammasome signaling, IRE1 and its downstream X-box binding protein 1 (XBP1) were activated in SCI tissues as well as in OGD neurons; while inhibition of IRE1 by STF-083010 in SCI rats or by si-RNA in OGD neurons suppressed inflammasome signaling and pyroptosis. Interestingly, the SCI/OGD-stimulated IRE1 activation was attenuated by CORM-3 treatment.

Interpretations: CO may alleviate neuron death and improve motor functional recovery in SCI through IRE1 regulation, and administration of CO could be a promising therapeutic strategy for SCI.

© 2018 Published by Elsevier B.V. This is an open access article under the CC BY-NC-ND license (<http://creativecommons.org/licenses/by-nc-nd/4.0/>).

1. Introduction

Traumatic spinal cord injury (SCI) is a devastating disease, leading to sensory disorders and physical disabilities [1]. The primary mechanical damage and the secondary sequential damage are the crucial pathophysiological features of SCI. The latter is orchestrated by a series of detrimental events such as inflammatory response, endoplasmic reticulum

(ER) stress, mitochondrial dysfunction and excitotoxicity [2–5]. Neurons are of vital importance for central nervous system (CNS), however they could not regenerate when impaired [6,7]. Due to the irreversibility of mechanical injury, alleviating the secondary neuron death and ameliorating the surviving neuronal function are considered as the key strategy for SCI therapy.

Heme oxygenase (HO) is a highly conserved enzyme involved in the secondary injury process, it degrades heme into biliverdin, carbon monoxide, and free iron (Fe^{3+}). Genetic or pharmacological upregulation of HO-1 activity preserves spinal cord function and restrains the neuron death after SCI [8–13]. As a heme degradation product, carbon monoxide (CO) has been proved to have various bioactivity such as anti-

* Corresponding authors.

E-mail addresses: spinexu@163.com (H. Xu), fengnq@163.com (N. Tian), zhangxiaolei@wmu.edu.cn (X. Zhang).

¹ Gang Zheng, Yu Zhan and Haoli Wang contributed equally to this work.

Research in context

Evidence before this study

Genetic or pharmacological regulation of HO are identified as potential therapeutic target for SCI. As a heme degradation product, although CO has various bioactivity such as anti-inflammatory, anti-apoptotic and antioxidant in low concentration, the role of CO in SCI is still unknown. Applying hemin or chemicals which may regulate HO expression or activity to increase CO production are inadequate to elaborate the direct role of CO in SCI.

Added value of this study

In this study, we demonstrated CORM-3 improved functional recovery and diminished the neuron death in the rat following SCI. Moreover, the SCI-induced neuronal pyroptosis occurrence and inflammasome signaling was inhibited by CORM-3.

Implications of all the available evidence

Our data suggest CORM-3 offer therapeutic benefit for SCI patients.

inflammatory, anti-apoptotic and antioxidant in low concentration [14–16], which might explains the HO-1-induced protection following SCI. However, the direct role of CO in SCI is still unknown.

Neuroinflammation plays a key role in the secondary phase of SCI after initial cell death. Activation of cytoplasmic inflammasome complexes is regarded as the essential step of neuroinflammation and a key trigger for neuron death called pyroptosis [17]. Unlike traditional apoptosis, pyroptosis is defined as an exceptional category of inflammatory necrosis, characterized by the cell swell, rupture, the pore formation in cell membrane and the release of cytosolic contents [18]. And growing evidences proved that pyroptosis contributes to neuron death in acute CNS injury, such as ischemic stroke, subarachnoid hemorrhage and traumatic injury of brain and spinal cord [17,19–23]. During the CNS damage, inflammasomes are activated by the danger signals including high extracellular K⁺, ATP, β -amyloid and subsequently induced the pyroptosis occurrence [9,22]. The process of inflammasomes-mediated pyroptosis is a complex cascade and still remains many unanswered doubts [24,25]. In brief, during the inflammasome signaling is primed and activated, the activated inflammasomes assembly binds and cleaves the pro-caspase1 to form active subunits, which further leads to inflammatory response and pyroptosis by activating the pro IL-1 β , pro IL-18, and Gasdermin D (GSDMD, pore forming protein) [22]. The pharmacologically or genetically suppression of inflammasomes signaling or direct ablation of caspase1 have been demonstrated the protection of neuron in brain and spinal cord injury model [23,26–29].

Several murine brain injured models demonstrated that delivering CO by inhalation or the exogenous CO donor, CO-releasing molecule (CORM)-3, suppresses neuroinflammation, blood-brain barrier disruption and promotes neurogenesis [30–32]. Except for the anti-inflammatory, anti-apoptotic and regenerative effects, recent studies implied that CO possesses regulatory effects on inflammasomes signaling and pyroptosis occurrence [33–35]. Nevertheless, the relationship between CO and inflammasome-stimulated pyroptosis in neuron was unknown in SCI.

In this study, we firstly measured CO content variation within 7 days following SCI, revealing that the CO content variation is consistent with the expression of HO-1 after SCI. Next, we showed that exogenously increasing CO by CORM-3 improved functional recovery and diminished

the neuron death in the rat model of SCI. Moreover, CORM-3 treatment attenuated pyroptosis occurrence and inflammasome priming in neuron *in vivo* and *in vitro*, the potential mechanism for CORM-3-regulated inflammasomes in SCI might be associated with abnormal activation of the kinase/endoribonuclease inositol-requiring enzyme (IRE1). This study demonstrates the direct role of CO in SCI, showing its potential as well as working mechanism for SCI therapy.

2. Materials and methods

2.1. Reagents and antibodies

Carbon monoxide releasing molecule 3 (CORM-3) and STF-083010 were purchased from Selleck (Houston, Texas, USA). Antibody against IL-1 β was purchased from R&D system (Minneapolis, Minnesota, USA). Antibody against NLRP1 was purchased from Cell Signaling Technology (Beverly, MA, USA). Antibodies against HO-1, caspase1, caspase11, IL-18, NLRP3, p-IRE1, IRE1, NeuN, GSDMD and GAPDH were the products of Abcam (Cambridge, MA, USA).

2.2. Animal and SCI model

Adult female Sprague–Dawley rats (220–250 g, 8-week old) were purchased from the Animal Center of the Chinese Academy of Sciences in Shanghai, China, housed in standard temperature conditions with a 12 h light/dark cycle and regularly fed with food and water. The protocol for animal care and use conformed to the Guide for the Care and Use of Laboratory Animals from the National Institutes of Health and was approved by the Animal Care and Use Committee of Wenzhou Medical University.

The rats were randomly divided into four groups. All rats were anesthetized by an intraperitoneal injection of sodium pentobarbital (65 mg/kg). Following shaved and sterilized in the back, the skin was incised along the midline of the dorsum to expose the vertebral column and a laminectomy was performed at the T9 level. The exposed spinal cord was subjected to crush injury by compression with a vascular clip (30 g force; Oscar, China) for 1 min. The same surgical procedure was performed in sham group rats, but there is no crush to the spinal cord is exposed for 1 min. Postoperative care involved manual urinary bladder emptying twice daily until the return of bladder function and the administration of cefazolin sodium (50 mg/kg, i.p.). And the rats experiencing the SCI were randomly divided into three groups, respectively, treatment with CORM-3 or iCORM-3 or saline. To confirm the CO effect, we prepared the inactive CORM-3 (iCORM-3), that was produced by leaving CORM-3 in saline (pH = 7.4) overnight at room temperature to allow all CO to be released from the molecule [34]. CORM-3 was diluted with normal saline and achieved a final CORM-3 concentration of 8 mg/ml. After surgery, the CORM-3 solution was immediately injected to tail veins with a dose of 8 mg/kg/day until the rats were sacrificed. Equivalent normal saline and iCORM-3 injections were administered for vehicle control. In addition, for IRE1 inhibitor experiment, the SCI rats were divided into two groups. The rats were immediately injected with STF-083010 (10 mg/kg/d) or DMSO after SCI, both given in 16% (vol/vol) Cremophor EL (Sigma-Aldrich) saline solution *via* i.p. injections. For pyroptosis inhibitor experiment, VX-765 (150 mg/kg/d; meilunbio, Da Lian, China) was dissolved in 20% cremophor and injected intraperitoneally in rats after SCI. All animals showed no significant side effects resulting from drug treatment such as mortality or signs of infectious disease during these experiments.

2.3. Locomotion recovery assessment

The Basso, Beattie, and Bresnahan (BBB) scores were assessed by three trained investigators who were blinded to experiment in an open-field scale at 1, 3, 7, 14, 21 and 28 days post-operation. Briefly, the BBB scores range from 0 points (complete paralysis) to 21 points

(normal locomotion). The scale was developed using the natural progression of locomotion recovery in rats with thoracic SCI [36]. Moreover, the footprint analysis was performed by dipping the rat's hindpaws with blue dye at 28 days after SCI. Ten rats for each group were used to assess the motor function.

2.4. Hematoxylin-Eosin staining and Nissl staining

The rats of each group ($n = 5$) were euthanized with an overdose of sodium pentobarbital, followed by 4% paraformaldehyde in 0.01 M phosphate buffered saline (PBS, pH = 7.4) at 7 days after SCI. Tissue segments containing the lesion (1 cm on each side of the lesion) were paraffin embedded. Transverse paraffin sections (5 μ m thick) were mounted on poly-L-lysine-coated slides for Hematoxylin-Eosin (HE) staining and Nissl staining and examined under a light microscope. The cellular stain HE was used to observe the cavity, at 5 mm from the lesion site. The measurements were reported as the percent of preserved area in relation to the total area of each section analyzed [37]. For Nissl staining, the number of ventral motor neuron (VMN) in sections were assessed as in previous report [38]. Transverse sections were collected at rostral, caudal 5 mm, and the lesion site and stained with cresyl violet acetate. After determination of the cells located in the lower ventral horn, cells larger than half of the sampling square (20 \times 20 μ m) were counted as a VMN. The cells above the line at 150 μ m ventral from the central canal were excluded. The cells were manually counted from each field using Metamorph software.

2.5. Carbon monoxide content detection

The CO content in spinal cord was detected with endogenous carbon monoxide assay kit (Nanjing Jiancheng Bioengineering Institute, Nanjing, China) as previously described [39,40]. The specific steps were conducted according to the manufacturer's instructions. Briefly, the spinal cord tissue samples were removed at 1,3,5,7 days after SCI. The spinal cord segment (0.5 cm length) at the contusion epicenter was dissected and homogenized in PBS. Mix 1 mL of Hb solution (0.25 mL of fresh-packed erythrocytes in 50 mL of ammonia solution) with 0.5 mL of a sample or an equivalent amount of water, which is used as a blank to measure the endogenous CO that presented in the Hb solution, vortex-mix and let stand for 10 min. Read the absorbance at 541 nm and 555 nm against a reference curvette containing water for three times and get the average. Then, the ratio(R) of the 541 to 555 readings was record and further to calculate the CO content in sample. Eight rats for each group were used to detect the CO change after SCI.

2.6. Primary neuron culture and treatment

Primary neurons were cultured as previously described [41]. Briefly, primary neurons were obtained from cerebral cortices of 17-day-old SD rat embryos, and cultured in Neuronal Basal medium containing 2% B27 and 1% L-glutamine in a humidified atmosphere of 5% CO₂ and 95% air at 37 °C. The medium was replaced every 2 days and cells were cultured for additional seven days before use. For OGD, the medium was replaced by glucose-free Dulbecco's Modified Eagle Medium, and placed in a hypoxic chamber containing 5% CO₂, 0.02% O₂ and 94.98% N₂ at 37 °C for 6 h. The CORM-3 (100 μ m) and STF-083010 (50 μ m) was pretreated (3 h) before OGD.

2.7. Small interfering RNA transfection

siRNA for rat IRE1 gene was purchased from Santa Cruz Biotechnology (sc-270028; Dallas, TX, USA). Neurons were seeded in a six-well plate and cultured for 24 h to 60–70% confluency. The cells were transfected with 50 nM negative control or siRNA duplexes using Lipofectamine 2000 siRNA transfection reagent (Thermo Fisher, UT, USA).

After the following further treatments, cells were harvested for western blot experiments.

2.8. LDH releasing assay

The supernatant from serum-free media was filtered using 0.2- μ m syringe filters to use for LDH release detection. The detection was using a commercially available kit (Solarbio, Beijing). One supernatant was transferred to 96-well plates, and then the reaction mixture was added and incubated in the dark for 30 min at RT. LDH concentration was quantified by measuring the absorbance at 490 nm.

2.9. ELISA

Spinal cord samples ($n = 5$) were homogenized in phosphate-buffered saline (PBS), subsequently centrifuged at 5000 \times g at 4 °C for 10 min. IL-1 β and IL-18 concentrations in the supernatant were detected using enzyme-linked immunosorbent assay (ELISA) kits (Thermo Fisher, UT, USA).

2.10. Real-time PCR

The total RNA was extracted from spinal cord by TRIzol reagent (Invitrogen, Grand Island, NY). One microgram of total RNA was used to synthesize cDNA (MBI Fermentas, Germany). For the quantitative realtime PCR (qPCR), a total 10 μ l of reaction volume was used, including 5 μ l of 2 \times SYBR Master Mix, 0.25 μ l of each primer and 4.5 μ l of diluted cDNA. Parameters of RT-PCR were: 10 min 95 °C, followed by 40 cycles of 15 s 95 °C and 1 min 60 °C. The reaction was performed using CFX96Real-Time PCR System (BioRad Laboratories, California, USA). The cycle threshold (Ct) values were collected and normalized to the level of GAPDH. The level of relative mRNA of each target gene was calculated by using the 2- $\Delta\Delta$ Ct method. The primer sequences were as follow: caspase1 (F) 5'-GACCGAGTGGTCCCTCAAG-3' and (R) 5'-GACGTGTACGAGTGGGTGTT-3'; IL-1 β (F) 5'-TGCTGACCCATGTGAGCTG-3' and (R) 5'-GCCACAGGGATTTGTGCTT-3'; IL-18 (F) 5'-ATATCGACCGAACAGCCAAC-3' and (R) 5'-TTCCATCCTTACAGATAGGG-3'; NLRP1 (F) 5'-GTGGCTGGACCTCTGTTGA-3' and (R) 5'-GGCGTTTCTAGGACCATCCC-3'; NLRP3 (F) 5'-CCAGAGCCTCACTGAACTGG-3' and (R) 5'-AGCATTGATGGGTCAGTCCG-3'; GAPDH (F) 5'-ATGACATCAAGAAGTGGTG-3' and (R) 5'-CATACCAGAAATGAGCTTG-3'.

2.11. Western blot analysis

RIPA lysis buffer (Beyotime, Shanghai, China) containing 1 mM PMSF was used to extract total protein followed by protein concentration measurement with an Enhanced BCA Protein Assay Kit (Beyotime, Shanghai, China) using a Microplate Reader (Molecular Devices Flexstation 3, USA). 40 ng of tissue protein was separated by sodium dodecylsulfate-polyacrylamide gel electrophoresis (SDS PAGE) and transferred to a polyvinylidene difluoride membrane (Bio-Rad, California, USA). After blocking with 5% nonfat milk for 2 h, the membranes were incubated with the primary antibody against HO-1 (1:500), GSDMD (1:500), caspase1 (1:1000), caspase11 (1:500), IL-1 β (1:500), IL-18 (1:200), NLRP1 (1:1000), NLRP3 (1:500), p-IRE1 (1:500), IRE1 (1:500), GAPDH (1:5000). Then, the membranes were washed with TBS for 5 min three times, and treated with horseradish peroxidase-conjugated secondary antibodies. After 3 times washing with TBST, the blots were visualized by electrochemiluminescence plus reagent (Invitrogen, Carlsbad, USA). Finally, the intensity of these blots were quantified with Image Lab 3.0 software (Bio-Rad, California, USA).

2.12. Immunofluorescence staining

Spinal cord tissue samples were obtained 3 days after injury. All spinal cords were postfixed in 4% PFA, washed, and embedded in paraffin.

Transverse sections of 5- μ m thickness were cut, deparaffinized in xylene, and rehydrated by ethanol washes. And the sections were incubated with 10% normal goat serum for 1 h at room temperature in PBS containing 0.1% Triton X-100. They were then incubated with the appropriate primary antibodies overnight at 4 °C in the same buffer. The following primary antibodies were used, based on differing targets: HO-1 (1:100), Caspase1 (1:100), NeuN (1:1000), p-IRE (1:100). After primary antibody incubation, sections were washed for 4 \times 10 min and then incubated with Alexa Fluor 488/594 goat anti-rabbit/mouse secondary antibodies for 1 h at room temperature. Sections were rinsed three times with PBS and incubated with 4,6-diamidino-2-phenylindole (DAPI) for 10 min and finally washed in PBS and sealed with a coverslip. The images were captured with a fluorescence microscope (Olympus Inc., Tokyo, Japan), positive neurons in each section were counted by three observers who were blinded to the experimental groups. The rates of Corresponding-protein positive cells per section was calculated from values obtained by counting 30–40 random sections throughout the lesion site of each animal, with five animals examined per group.

2.13. Statistical analysis

The results were presented as mean \pm S.D. Statistical analyses were performed using SPSS statistical software program 20.0 (IBM, Armonk, NY, USA). Data were analyzed by one-way analysis of variance (ANOVA) followed by Tukey's test for comparison between control and treatment groups. BBB score data were analyzed by Mann-Whitney test. $P < .05$ was considered statistically significant.

3. Results

3.1. CO content varies in spinal cord tissues after SCI

We detected the expression of HO-1, which is the most pivotal enzymes of autogenous CO generation [42], at 1, 3, 5 and 7 days after SCI. The western blotting results revealed the time course of HO-1 expression level increased at 1 day after SCI, declined at 3 days and then gradually tended to be stabilized at 5 and 7 days (Fig. 1A). By immunofluorescence double staining, we observed that the HO-1 mainly colocalized with neuron in injured spinal cord (Fig. 1B). To ascertain the change of CO level after SCI, we quantify the CO content in spinal cord at the same post-SCI time points; the results showed that the time course of CO concentration is basically consistent with the HO-1 expression after SCI (Fig. 1C). These results indicated that endogenous CO and HO-1 expression in spinal cord was increased after SCI.

3.2. CORM-3 contributes to increased CO content in spinal cord tissues

When SCI model was established in rats, the water-soluble exogenous CO donor, CORM-3, was continuously applied on SCI; meanwhile the inactive CORM-3 (iCORM-3), which does not release CO, was taken as the negative control. The results showed that CORM-3 administration efficiently multiplied CO content in the spinal cord tissues at 1 day post-SCI (Fig. 1C). Although the CO concentration in CORM-3 group appeared to decline slightly after 1 day, its total level was prominently higher than the iCORM-3 group (Fig. 1C). Meanwhile, there was no significant discrepancy in CO content among the SCI group and iCORM-3 group (Fig. 1C).

3.3. SCI-mediated neuron loss and neurological deficits are alleviated by CORM-3 treatment

To investigate whether CO exerted a protective effect on the SCI, the BBB scores and footprint analysis were executed to assess the recovery of motor function in different groups. As shown in Fig. 2A, the BBB scores of rats in the Sham group maintained at the maximum score of 21, while the score of rats suffering from SCI dropped immediately to 0 points at

1 day after surgery. Compared to the SCI group and iCORM3 group, rats in CORM-3 treatment group exhibited significant promoted locomotor restoration, as indicated by increased BBB score at 7, 14, 21, 28 days after injury (Fig. 2A). Meanwhile, the footprint vividly showed the gait of the rat's hind limb, was performed at 28 days post SCI. The results appeared as a wavy line in SCI and iCORM-3 group, suggesting the hind limb in the rats of groups above lost its function of supporting body weight and coordinating forelimb movement (Fig. 2B). We also analyzed step length and stride width of footprint. As shown in Fig. S1A&B, rats with SCI exhibits shorter step length and longer stride width relative to the sham group, however CORM-3 treatment ameliorated this phenomenon. Nevertheless, we can found obvious paw prints along with harmonized alternate gait in rats of CORM-3 group (Fig. 2B).

Histomorphological differences were accessed by HE staining. As shown in Fig. 2C & D, CORM-3 treatment decreased the size of the lesion cavity at 7 days post SCI. We also applied Nissl staining to detect neuronal survival at 3 days after SCI. The counting analysis of Nissl staining revealed that CORM-3 injection increased the number of ventral motor neuron (VMN) as compared to the SCI non-treatment and iCORM treatment (Fig. 2C, E). Interestingly, there is no significant difference in the results of the BBB scores, footprint, HE staining and Nissl staining between the SCI group and the iCORM-3 group, suggesting that the protective effects of CORM-3 on SCI was based on its CO donor capability.

3.4. CORM-3 inhibites pyroptosis and inflammasome expression following SCI

Unlike other types of cell death, pyroptosis is redefined as gasdermin-mediated programmed necrotic cell death which depends on caspase1 or caspase11/4/5 activation, leading to IL-1 β and IL-18 stimulation, cytomembrane pore formation and subsequently the release of inflammatory mediators and cellular contents [18,43–45]. Rats treated with VX-765, the classical pyroptosis inhibitor, has a higher BBB scores at 7 days after SCI relative to the SCI group (Fig. S1C). Although it is controversial about which death form, namely apoptosis, pyroptosis and necrosis dominates the acute stage of central nervous system (CNS) injury, pharmacological or genetical suppression of pyroptotic death has been proved to be a potential therapeutic target for CNS injury [9,20,27]. Previous studies have reported the anti-apoptotic effect of CO in *in vitro* and *in vivo* models of traumatic brain injury (TBI) [31], however the effect of CO on pyroptosis in CNS is unknown.

We firstly measured the mRNA level of pyroptosis-related key genes at different time points after SCI. The mRNA level of caspase1 elevated at 1 day after SCI, peaked at 3 days and persisted at the high level at 7 days; the expression of IL-1 β and IL-18 showed the similar pattern (Fig. 3A). Next, we analyzed the pyroptosis level in spinal cord tissues by western blot and immunofluorescence. Immunofluorescence double staining of cleaved-caspase1 and NeuN showed that cleaved-caspase1 positive neuron in spinal cord anterior horn was lessen by CORM-3 administration following SCI (Fig. 3B). As shown in Fig. 3C & D, CORM-3 reversed the increased expression of GSDMD, cleaved-caspase1, cleaved-caspase11, IL-1 β and IL-18 induced by SCI; the expression of IL-1 β and IL-18 had further been confirmed by ELISA analysis (Fig. 3E).

In physiological conditions, caspase1 presents as inactive precursor in the cytoplasm; however in pathological conditions, it could be cleaved by inflammasome to produce a tetramer consisting of active subunits [17]. Our PCR results showed that the time course of the NLRP1 and NLRP3 mRNA expression was broadly consistent with caspase1 after SCI (Fig. 3F), suggesting pyroptosis was correlated with inflammasome signaling in SCI. The western blot analysis also showed that the expression of NLRP1 and NLRP3 in spinal cord lysate was ascended following SCI, whereas CORM-3 reversed these trends, suggesting the priming step of inflammasome signaling was inhibited by CORM-3 treatment (Fig. 3G, H). The priming of inflammasome signaling is accompanied by the synthesis of pro-IL-1 β and pro-IL-18. As shown in

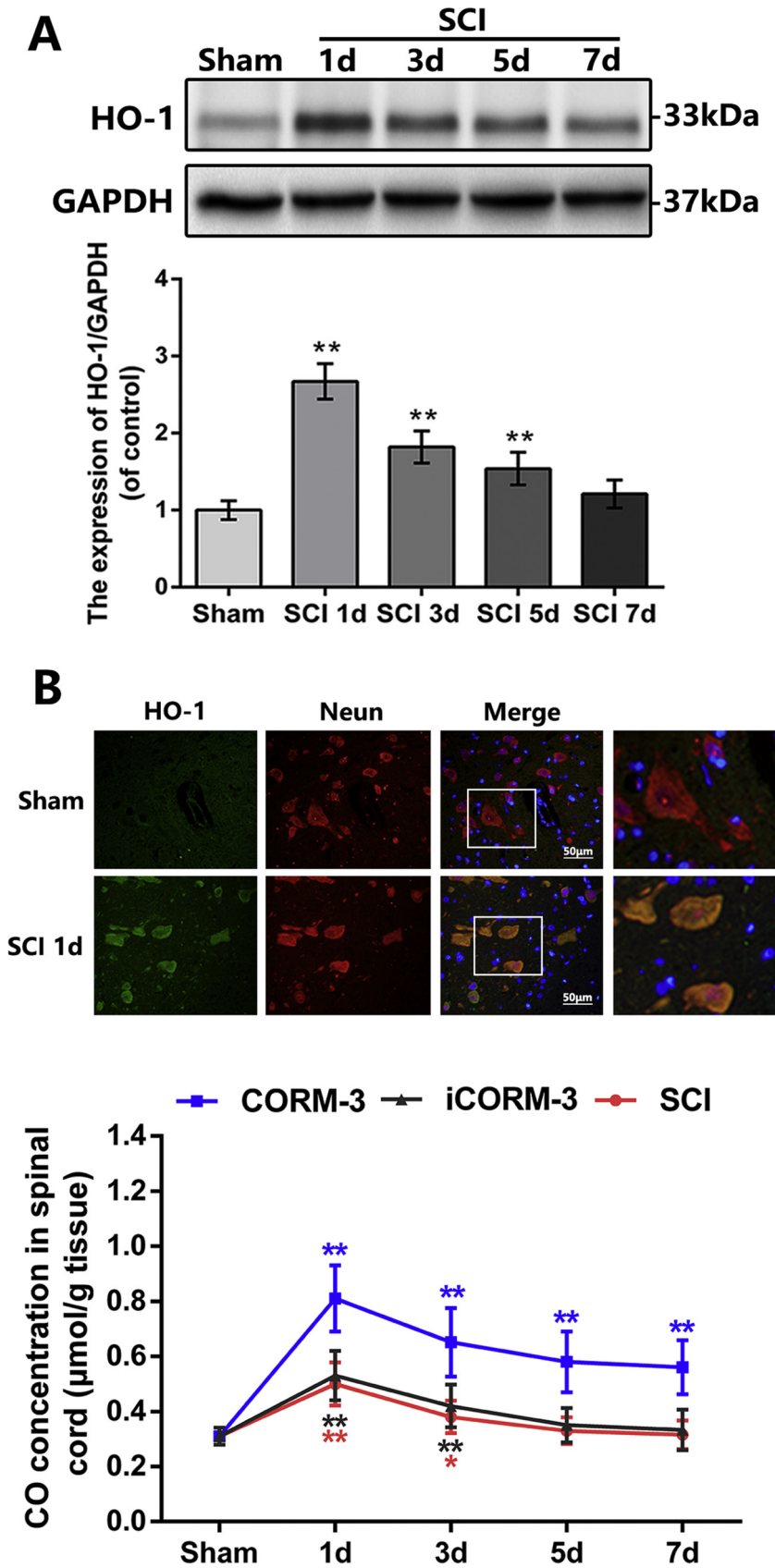


Fig. 1. Carbon monoxide content and HO-1 expression in the early stages after SCI. (A) The protein expression of HO-1 in spinal cord at early time points after SCI ($n = 5$). (B) Double immunofluorescence of HO-1 and NeuN in sections from tissue at 1 day after SCI (bar: 50 μm) ($n = 5$). (C) Carbon monoxide concentration at early time points after SCI ($n = 10$). All data represent mean \pm S.D. ($n = 5$). ** $P < .01$.

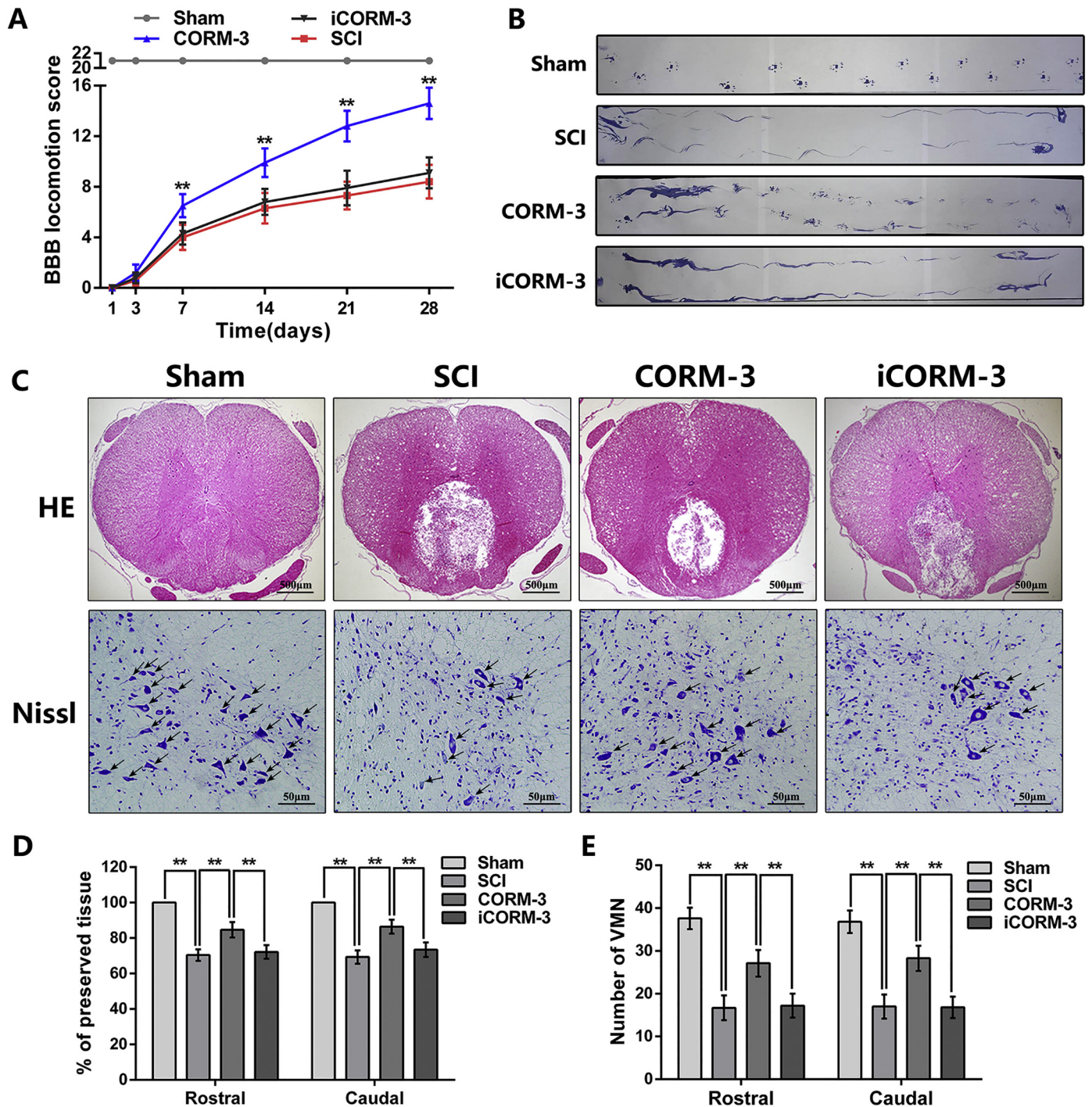


Fig. 2. CORM-3 attenuate neuron death and improve functional recovery after SCI. (A) The Basso, Beattie and Bresnahan (BBB) scores of each group ($n = 10$). (B) The footprint result of each group ($n = 10$). (C) The HE staining at 7 days post SCI (bar: 500 μm) and Nissl staining at 3 days (bar: 50 μm). (D) The percent of preserved tissue in relation to the transverse area of the spinal cord by HE staining ($n = 5$). (E) Counting number of VMN by Nissl staining ($n = 5$). All data represent mean \pm S.D. ** $P < .01$.

Fig. S1E&F and S1J&K, CORM-3 treatment down-regulated the SCI-upregulated expression of pro-IL-1 β , pro-IL-18 and cleaved GSDMD.

These results suggest that CORM-3 inhibit pyroptosis and inflammasome signaling priming following SCI in rats.

3.5. CORM-3 suppresses SCI-induced IRE1 phosphorylation in neuron *in vivo*

CO has emerged various bioactivities in multiple disease models [14,15]; however, the specific molecular target for CO is still not clear. Early researches mainly focus on the regulation of ion channels

[46–48]; recently, researchers found that thapsigargin or tunicamycin (the classical agonist of ER stress) induced IRE1 phosphorylation was blocked by CORMs pretreatment [14,49,50], indicating CORM-3 may regulate ER stress. In our study, we examined the IRE1 phosphorylation level and its downstream protein XBP1s expression by western blot (Fig. 4A, B). And we demonstrated that CORM-3 treatment inhibited the SCI-mediated IRE1-XBP1 pathway stimulation. Moreover, we showed that p-IRE1 α was mainly localized in neurons as indicated by the immunofluorescence analysis in spinal cord tissues (Fig. 4C). The green fluorescence intensity in neuron was increased in SCI group relative to the sham group, CORM-3 alleviated this phenomenon. These

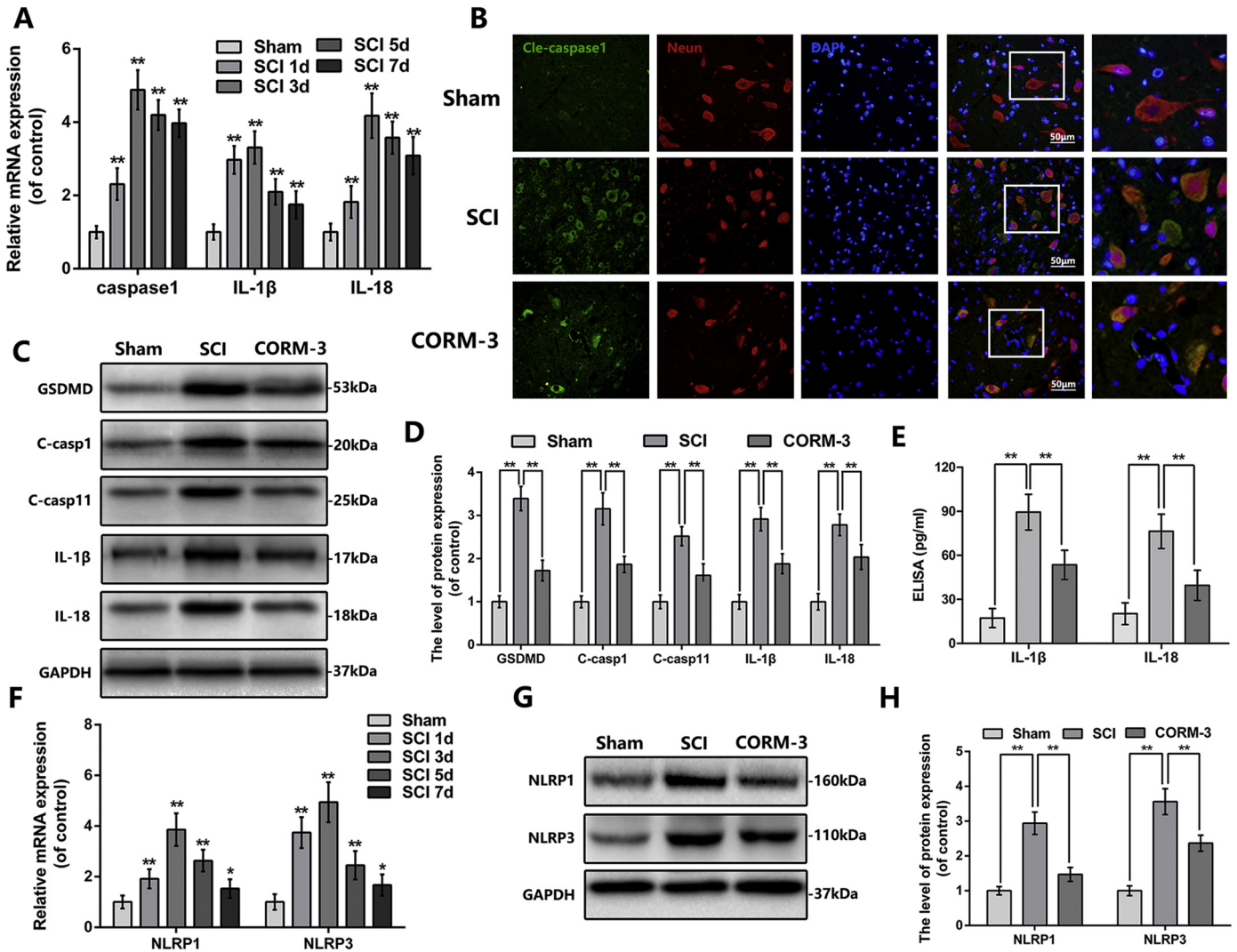


Fig. 3. CORM-3 inhibit pyroptosis and inflammasomes signaling at 3 days after SCI. (A) The mRNA expression of caspase1, IL-1 β and IL-18 of each group at early time points after SCI. (B) Double immunofluorescence of cleaved-caspase1 and NeuN in sections from tissue at 3 day after SCI (bar: 50 μ m) (C) and (D) The protein expression of GSDMD, cleaved-caspase1, cleaved-caspase11, IL-1 β and IL-18 in spinal cord at 3 days after SCI. (E) The ELISA of IL-1 β and IL-18 at 3 days after SCI. (F) The mRNA expression of NLRP1 and NLRP3 of each group at early time points after SCI. (F) and (G) The protein expression of NLRP1 and NLRP3 in spinal cord at 3 days after SCI. All data represent mean \pm S.D. ($n = 5$) $^{**}P < .01$.

results suggest that CORM-3 suppress SCI-induced IRE1 phosphorylation in neuron.

3.6. CORM-3 restrains the IRE1 phosphorylation and inflammasome expression in OGD neuron *in vitro*

To further explain the working mechanism of CO-dependent protective effects on SCI, we exposed the primary neurons at OGD condition to mimic SCI model *in vitro* [31,51]. Interestingly, the suppression of IRE1 phosphorylation by CORM-3 was only observed at the neuron under OGD condition, and treated of neuron with CORM-3 alone had no significant effect on p-IRE1 and IRE1 expression (Fig. 5A, B). Consistent with our *in vivo* experiments results, CORM-3 treatment down-regulated the OGD-induced GSDMD, cleaved-caspase1, IL-1 β , NLRP1 and NLRP3 expression in neuron (Fig. 5E-G). These results suggest that CORM-3 restrain the IRE1 phosphorylation and inflammasome expression in neuron after OGD.

3.7. Inhibition of IRE1 blocks inflammasome priming in OGD neuron *in vitro*

Based on the phenomena above, we questioned if OGD-induced IRE1 activation involves in inflammasome signaling and pyroptosis

occurrence. Therefore, we transfected neuron with IRE1-siRNA, the knock-down efficiency was confirmed by western blot (Fig. 5C). As shown in Fig. 5E-G, IRE1 inhibition by siRNA interdicted GSDMD, cleaved-caspase1, IL-1 β , NLRP1 and NLRP3 expression in OGD-exposed neuron. Furthermore, administering STF-083010, the specific antagonist of IRE1, to OGD-exposed neuron showed the similar results to IRE1-siRNA knock down (Fig. 6G, H). These results showed that inhibition of IRE1, either genetically by siRNA or pharmacologically by STF-083010, blocks regulatory effects of CORM-3 on inflammasome in OGD neuron *in vitro*, indicating the regulatory effects of CORM-3 on inflammasome is through IRE1.

3.8. Pharmacological inhibition of IRE1 relieves inflammasome priming, activation and pyroptosis following SCI *in vivo*

To further confirm the effect of IRE1 signaling in SCI, we applied STF-083010 in rat SCI model. The western blot demonstrated that STF-083010 markedly inhibited the IRE1 phosphorylation following SCI (Fig. 6A). As shown in Fig. 6B, the fluorescence intensity of cleaved-caspase1 in neuron was reduced by STF-083010 administration post-SCI. By western bot results, the expression of GSDMD, cleaved GSDMD, cleaved-caspase1, cleaved-caspase11, IL-1 β , IL-18, NLRP1,

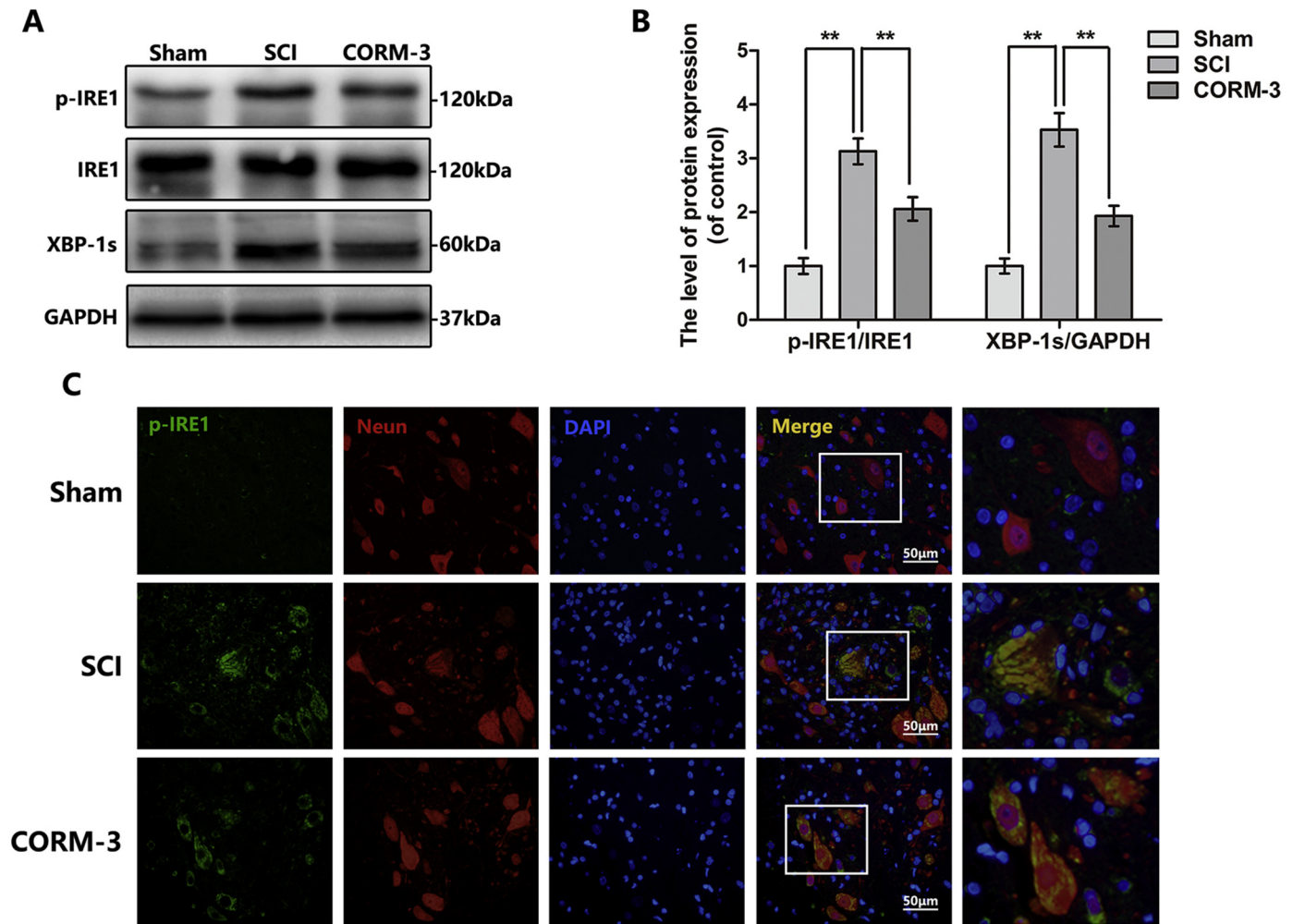


Fig. 4. CORM-3 restrains IRE1/XBP-1 s pathway at 3 days after SCI. (A) and (B) The protein expression of p-IRE1, IRE1 and XBP-1 s in spinal cord at 3 days after SCI. (C) Double immunofluorescence of p-IRE1 and NeuN in sections from tissue at 3 days after SCI (bar: 50 μ m). All data represent mean \pm S.D. ($n = 5$). ** $P < .01$.

NLRP3, pro-IL-1 β and pro-IL-18 were observed downregulated in STF-083010 treatment group (Fig. 6C-F and Fig. S1G-K). Together, these results suggest that pharmacological inhibition of IRE1 by STF-083010 relieves inflammasome priming and pyroptosis following SCI *in vivo*.

4. Discussion

As a product of haem degradation, CO has been demonstrated to have various biological functions such as anti-inflammatory, anti-apoptotic and anti-oxidative effects at low concentration [15,46]. Recently, it was reported that CO could prevent pericyte apoptosis following TBI [31]. We are the first to report that the dynamic change of CO content in spinal cord at the early stage of SCI and the role of CORM-3 in neuron death and functional recovery following SCI. Moreover, we further demonstrated the protective effects of CORM-3 might be through the regulation of IRE1-inflammasome pathway.

General dogma showed CO is poisonous, because of its high affinity with Hb. Therefore, we administered CORM-3 *via* tail vein thereby avoiding traditional pulmonary delivery systems, which greatly reduce the toxicity of CO. Prabhu et al. administered CORM-3 (40 mg/kg/d) to mice *via* intraperitoneal injections and found that a fairly constant level of carboxyhemoglobin (COHb; 6%) was maintained during the 24 days medication period, which is a safe concentration [16].

During the SCI process, the mechanical impact on spinal cord causes vascular rupture and tissue destruction which may subsequently enhance haem production (deriving from the dying cells or hemoglobin

[52,53]. Meanwhile, the expression and activity of HO-1 were up-regulated relative to the uninjured spinal cord [46]. These phenomena may explain SCI-induced CO content change in spinal cord.

The intervention of secondary injury-induced neuron death has been widely studied and identified as a potential therapeutic target for SCI. Besides apoptosis and necrosis (the traditional cell death categories), recent findings showed that a special death mechanism (pyroptosis) involves in the SCI pathology, which has been redefined as gasdermin-mediated programmed necrotic cell death. It is characterized by the following: [1] formation of discrete 1 to 2 nm pores in the plasma membrane with the cytolysis; [2] maturation and release of inflammatory cytokines such as IL-1 β and IL-18; [3] without mitochondrial ultrastructure damage; [4] a caspase3/6/7 independent cell death [22,23,25,45]. We found cleaved-caspase 1, cleaved-caspase 11, IL-1 β and IL-18 expression in spinal cord are increased after injury, suggesting pyroptosis is induced in SCI; while CORM-3 treatment could suppress it.

As a multiprotein complex initiating caspase 1 activation, inflammasome mainly consists of sensor Nod-like receptors (NLRs), adaptor protein apoptosis-associated speck-like protein containing a caspase-activating recruitment domain protein (ASC), and pro-caspase 1 [21]. According to the NLR protein distinction, inflammasomes can be divided into different types, such as NLRP1, NLRP2, NLRP3, NLRP6, NLRP7 *et al.*, neuron in the spinal cord mainly express NLRP1 and NLRP3 [22]. Interestingly, NLRP1 inflammasome in neurons differs from that in macrophages in that it also contains caspase 11 and the inhibitor of apoptosis protein X-linked inhibitor of apoptosis protein

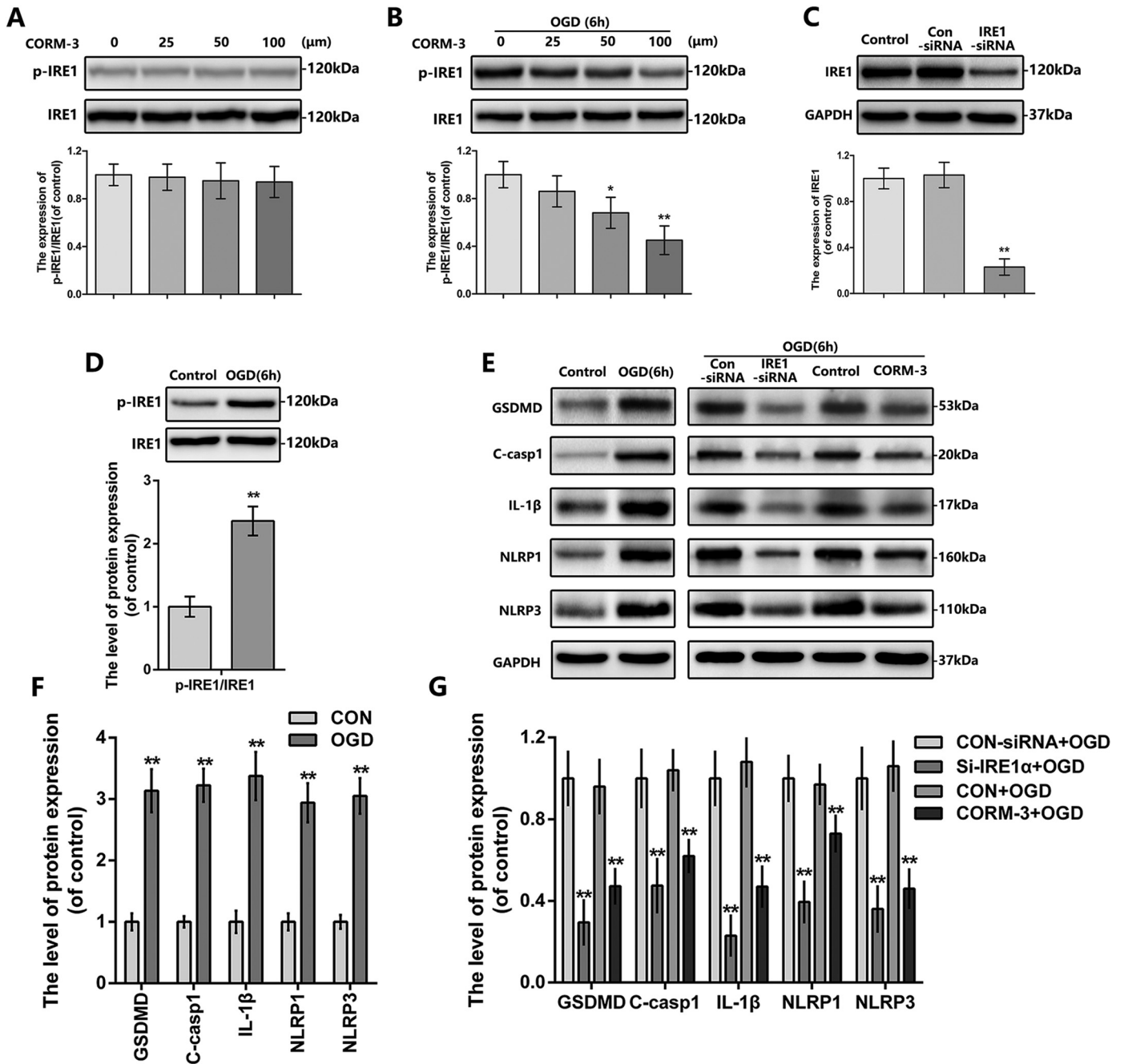


Fig. 5. The effect of CORM-3 and IRE1 in neuron under OGD condition. (A) and (B) The protein expression of p-IRE1 and IRE1 in neuron treated as above. (C) The protein expression of IRE1 in neuron treated as above. (D-G) The protein expression of p-IRE1, IRE1, GSDMD, cleaved-caspase1, IL-1 β , NLRP1 and NLRP3 in neuron treated as above. All data represent mean \pm S.D. ($n = 5$). ** $P < .01$.

(XIAP) [22,23,54]. The mechanism of caspase 11 activation in the CNS injury is still unknown. Whether NLRP1 inflammasome activation induced the cleavage of caspase 11 or whether caspase 11 forms its own inflammasome (independent of caspase 1) remains to be investigated [22]. Besides the canonical inflammasome pathways, caspase 11 could also be activated by other noncanonical inflammasome pathways [42]. For instance, during the bacterial infection, LPS in cytoplasm could cleavage caspase 11 [55,56].

The regulation of inflammasome is a multifactor involved process. Our study confirmed that the expression of NLRP1, NLRP3, pro-IL-1 β and pro-IL-18 are elevated in spinal cord after SCI, suggesting NLRP1 and NLRP3 inflammasome signaling are priming in SCI. As an acute sterile injury, inflammasome priming in SCI is triggered by the interactions between the danger/damage-associated molecular patterns (DAMPs)

and pattern recognition receptors (PRRs) [57–59]. DAMPs in CNS refers to those endogenous ligands such as high plasma glucose, β -amyloid, uric acid, K^+ and ATP that released by dying or dysfunctional cells, these ligands may be discerned by PRRs e.g. toll-like receptors, C-type lectin receptors, rig-like receptors, and NLRs [22,60].

The signaling pathways involving in injury stimulated inflammasome signaling in the CNS have not been well demonstrated yet, only the mechanism of K^+ efflux and ATP releasing has been described. After injury, the released ATP may activate P2X4 and P2X7 purinergic receptors, which may further facilitate K^+ efflux into extracellular space [22,25]. Meanwhile, high concentration of extracellular K^+ opens the pannexin (PANX1) channels which may result in ATP release and further stimulates P2X7 receptors and forms the interaction with inflammasomes [24,29]. This positive feedback involving P2X7

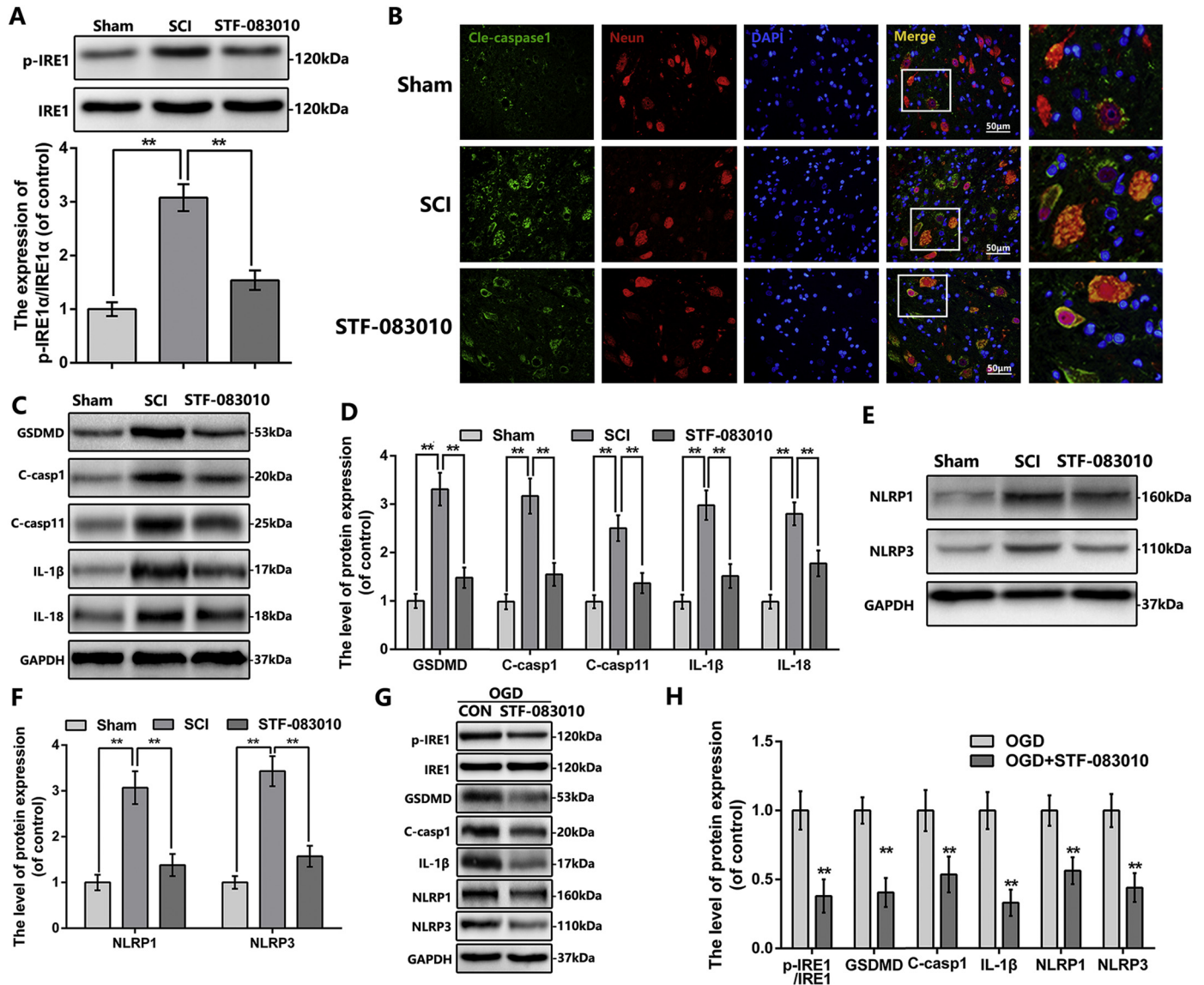


Fig. 6. STF-083010 suppress the inflammasome signaling and pyroptosis after SCI and OGD-induced neuron. (A) The protein expression of p-IRE1 in spinal cord at 3 days after SCI. (B) Double immunofluorescence of cleaved-caspase1 and NeuN in sections from tissue at 3 days after SCI (bar: 50 μ m). (C–F) The protein expression of GSDMD, cleaved-caspase1, IL-1 β , IL-18, NLRP1 and NLRP3 in spinal cord at 3 days after SCI. (G) and (H) The protein expression of p-IRE1, IRE1, cleaved-caspase1, IL-1 β , NLRP1 and NLRP3 in neuron treated as above. All data represent mean \pm S.D. ($n = 5$). ** $P < .01$.

receptors and P2X1 channels may decrease intracellular K⁺ concentration and triggers NLRP1 and NLRP3 inflammasome activation [21,22,25,54]. Until recently, P2X receptors are identified as the only ligand-gated ion channels regulated by CO [47,48]. However, there is no *in vivo* or *in vitro* evidence supporting that CO could inhibit P2X4 and P2X7 receptors in the presence of ATP. Wilkinson et al. demonstrated that CORM-2, another CO donor, is an efficient inhibitor of P2X4 receptor [48,61]; therefore, we speculate that CORM-3 might exert the same effect on P2X4 receptors, which of course needs further verification.

Misawa et al. reported that spatial arrangement of mitochondria may promote activation of the NLRP3 inflammasome [62]. The NLRP3 inflammasome may also respond to mitochondrial stress such as reactive oxygen species (ROS) and oxidized mitochondrial DNA [63]. While ROS overproduction, which is mainly derived from dysfunctional mitochondria, may result in dissociated thioredoxin-interacting protein (TXNIP) from thioredoxin, binding to NLRP3 so as to form active inflammasome complex [63,64]. These studies suggest that inflammasome activation is also closely related to mitochondria

function. CO has been reported to control mitochondrial quality via regulating mitochondrial biogenesis and mitophagy [33]. Therefore, the protective effect of CO against mitochondrial stress might provide a potential interpretation of inflammasome signaling by CORM-3.

The kinase/endoribonuclease inositol-requiring enzyme 1 (IRE1) is a pivotal endoplasmic reticulum (ER)-resident protein folding sensor, it is well known for its RNase activity that may degenerate ER-bound mRNA through activating X-box binding protein-1 (XBP1). And, it was also found to participate in NLRP1 and NLRP3 inflammasomes signaling [65,66]. Our results show that IRE1 phosphorylation level is elevated in rat SCI and neuron OGD model, accompanied by increased NLRP1/3 inflammasomes production and pyroptosis activity, whereas CORM-3 intervention reversed these changes. These results suggest that IRE1 may be involved in the regulation of CORM-3 on inflammasomes and pyroptosis. In an effort to explicate the role of IRE1 in SCI, we applied STF-083010, an IRE1 inhibitor, in SCI rats. Our results showed that SCI-induced GSDMD expression, caspase 1/11 cleavage, IL-1 β and IL-18 production and NLRP1/3 inflammasomes priming was alleviated after STF-083010 treatment, suggesting that CORM-3 may regulate

inflammasomes signaling and pyroptosis through IRE1. However, how CORM-3 regulates IRE1 is still unknown. Chung et al. reported that CO may reverse TG (classical ER stress stimulator)-induced IRE1 phosphorylation via upregulating PERK phosphorylation [49,67,68]. Also, they found that CO-mediated PERK phosphorylation is ROS dependent and is abolished by ROS scavenger *N*-acetyl-L-cysteine (NAC) [68]. Whether CORM-3 regulates IRE1 through the same mechanism in SCI needs further verification.

In conclusion, the present study reports that exogenous administration of CORM-3 increase the concentration of CO in spinal cord tissues, and CORM-3 treatment could alleviate neuron pyroptosis after spinal cord injury, the mechanism may related to IRE1 mediated inflammasome signaling regulation. Our study suggests that CO may be beneficial for SCI recovery and CORM-3 could be a potential agent for SCI therapy.

Supplementary data to this article can be found online at <https://doi.org/10.1016/j.ebiom.2018.12.059>.

(A) Representative footprint picture of each group ($n = 10$). (B) The footprint analysis of each group ($n = 10$). (C) The Basso, Beattie and Bresnahan (BBB) scores of each group ($n = 8$). We applied the VX-765 to rats following SCI to assess the functional role of pyroptosis in our SCI model. (D) The LDH release assays in the cell culture supernatant and the cells were treated as above ($n = 5$). (E–H) The protein expression of pro-IL-1 β and pro-IL-18 in spinal cord at 3 days after SCI ($n = 5$). (I) Carbon monoxide concentration at 1,2,3 days after SCI and rats in each groups were treated as above ($n = 5$). (J) and (K) The protein expression of cleaved GSDMD in spinal cord at 3 days after SCI ($n = 5$). All data represent mean \pm S.D. ($n = 5$). * $P < .05$, ** $P < .01$.

Acknowledgement

This study is supported by National Natural Science Foundation of China (81601963, 81873992, 81572227); Wenzhou Science and Technology Bureau Foundation (Y20170083, Y20170092).

Author contributions

GZ wrote the paper, performed the experiments and generated data; GZ, WHZ and YZ performed the experiments and generated data; ZCL, FHZ and YFZ analyzed data; YSW, YLZ and SW contributed reagents and materials tools; YW conceived and designed the experiments; CX and GHX performed the supplemental experiments and generate data; HZX, NFT and XLZ designed the experiments and helped write the manuscript.

Author disclosure statement

The authors declare no competing financial interest.

References

- Agostinello J, Battistuzzo CR, Skeers P, Bernard S, Batchelor PE. Early spinal surgery following thoracolumbar spinal cord injury: process of care from trauma to theatre. *Spine* 2016;42(10):E617.
- Liu S, Sarkar C, Dinizo M, et al. Disrupted autophagy after spinal cord injury is associated with ER stress and neuronal cell death. *Cell Death Dis* 2015;6(1):e1582.
- Beattie MS, Hermann GE, Rogers RC, Bresnahan JC. Cell death in models of spinal cord injury. *Prog Brain Res* 2002;137:37.
- Di GS, Knoblich SM, Brandoli C, Aden SA, Hoffman EP, Faden AI. Gene profiling in spinal cord injury shows role of cell cycle in neuronal death. *Ann Neurol* 2003;53(4):454.
- Park E, Velumian AA, Fehlings MG. The role of excitotoxicity in secondary mechanisms of spinal cord injury: a review with an emphasis on the implications for white matter degeneration. *J Neurotrauma* 2004;21(6):754–74.
- O'Shea TM, Burda JE, Sofroniew MV. Cell biology of spinal cord injury and repair. *J Clin Invest* 2017;127(9):3259–70.
- Liu XZ, Xu XM, Hu R, et al. Neuronal and glial apoptosis after traumatic spinal cord injury. *J Neurosci* 1997;17(14):5395–406.
- Lin W, Wang S, Yang Z, et al. Heme oxygenase-1 inhibits neuronal apoptosis in spinal cord injury through down-regulation of Cdc42-MLK3-MKK7-JNK3 axis. *J Neurotrauma* 2017;34(3).
- Lin WP, Xiong GP, Lin Q, et al. Heme oxygenase-1 promotes neuron survival through down-regulation of neuronal NLRP1 expression after spinal cord injury. *J Neuroinflammation* 2016;13(1):52.
- Wei W, Shurui C, Zipeng Z, et al. Aspirin suppresses neuronal apoptosis, reduces tissue inflammation, and restrains astrocyte activation by activating the Nrf2/HO-1 signaling pathway. *NeuroReport* 2018;1.
- Lu T, Wu X, Wei N, et al. Lipoxin A4 protects against spinal cord injury via regulating Akt/nuclear factor (erythroid-derived 2)-like 2/heme oxygenase-1 signaling. *Retour Au Numéro* 2018;97:905.
- Diaz-Ruiz A, Maldonado PD, Mendez-Armenta M, et al. Activation of heme oxygenase recovers motor function after spinal cord injury in rats. *Neurosci Lett* 2013;556(1):26–31.
- Yamauchi T, Lin Y, Sharp FR, Noble-Haueslein LJ. Hemin induces heme oxygenase-1 in spinal cord vasculature and attenuates barrier disruption and neutrophil infiltration in the injured murine spinal cord. *J Neurotrauma* 2004;21(8):1017–30.
- Kim KM, Pae HO, Zheng M, Park R, Kim YM, Chung HT. Carbon monoxide induces heme oxygenase-1 via activation of protein kinase R-like endoplasmic reticulum kinase and inhibits endothelial cell apoptosis triggered by endoplasmic reticulum stress. *Circ Res* 2007;101(9):919–27.
- Motterlini R, Otterbein LE. The therapeutic potential of carbon monoxide. *Nat Rev Drug Discov* 2010;9(9):728–43.
- Wang G, Hamid T, Keith RJ, et al. Cardioprotective and antiapoptotic effects of heme oxygenase-1 in the failing heart. *Circulation* 2010;121(17):1912–25.
- Wei L, Chen Y, Jiao M, et al. Ablation of caspase-1 protects against TBI-induced pyroptosis in vitro and in vivo. *J Neuroinflammation* 2018;15(1):48.
- Wang Y, Gao W, Shi X, et al. Chemotherapy drugs induce pyroptosis through caspase-3 cleavage of a gasdermin. *Nature* 2017;547(7661):99.
- Adamczak SE, Vaccari JPDR, Dale G, et al. Pyroptotic neuronal cell death mediated by the AIM2 inflammasome. *J Cereb Blood Flow Metab* 2014;34(4):621–9.
- Fann YW, Lee SY, Manzanero S, et al. Intravenous immunoglobulin suppresses NLRP1 and NLRP3 inflammasome-mediated neuronal death in ischemic stroke. *Cell Death Dis* 2013;4(9):e790.
- Trendelenburg G. Molecular regulation of cell fate in cerebral ischemia: role of the inflammasome and connected pathways. *J Cereb Blood Flow Metab* 2014;34(12):1857–67.
- Vaccari JPDR, Dietrich WD, Keane RW. Activation and regulation of cellular inflammasomes: gaps in our knowledge for central nervous system injury. *J Cereb Blood Flow Metab* 2014;34(3):369–75.
- Vaccari JPDR, Lotocki G, Marcillo AE, Dietrich WD, Keane RW. A molecular platform in neurons regulates inflammation after spinal cord injury. *J Neurosci* 2008;28(13):3404–14.
- Zhou K, Shi L, Wang Y, Chen S, Zhang J. Recent advances of the NLRP3 inflammasome in central nervous system disorders. *J Immunol Res* 2016;2016(2):1–9.
- Walsh JG, Muruve DA, Power C. Inflammasomes in the CNS. *Nat Rev Neurosci* 2014;15(2):84–97.
- Zendedel A, Johann S, Mehrabi S, et al. Activation and regulation of NLRP3 inflammasome by intrathecal application of SDF-1 α in a spinal cord injury model. *Mol Neurobiol* 2016;53(5):3063–75.
- Wu J, Li M, Fan H, Zhou S, Zhu L. Targeting the NLRP3 inflammasome to attenuate spinal cord injury in mice. *J Neuroinflammation* 2017;14(1):207.
- Vaccari JPDR, Lotocki G, Alonso OF, Bramlett HM, Dietrich WD, Keane RW. Therapeutic neutralization of the NLRP1 inflammasome reduces the innate immune response and improves histopathology after traumatic brain injury. *J Cereb Blood Flow Metab* 2009;29(7):1251–61.
- Zendedel A, Mönning F, Hassanzadeh G, et al. Estrogen attenuates local inflammasome expression and activation after spinal cord injury. *Mol Neurobiol* 2017;55(2):1–12.
- Zeynalov E, Doré S. Low doses of carbon monoxide protect against experimental focal brain ischemia. *Neurotox Res* 2009;15(2):133.
- Choi YK, Maki T, Mandeville ET, et al. Dual effects of carbon monoxide on pericytes and neurogenesis in traumatic brain injury. *Nat Med* 2016;22(11):1335–41.
- Wang J, Di Z, Fu X, et al. Carbon monoxide-releasing molecule-3 protects against ischemic stroke by suppressing neuroinflammation and alleviating blood-brain barrier disruption. *J Neuroinflammation* 2018;15(1):188.
- Suliman HB, Piantadosi CA. Mitochondrial quality control as a therapeutic target. *Pharmacol Rev* 2016;68(1):20–48.
- Zhang W, Tao A, Lan T, et al. Carbon monoxide releasing molecule-3 improves myocardial function in mice with sepsis by inhibiting NLRP3 inflammasome activation in cardiac fibroblasts. *Basic Res Cardiol* 2017;112(2):16.
- Wang P, Huang J, Li Y, et al. Exogenous carbon monoxide decreases sepsis-induced acute kidney injury and inhibits NLRP3 inflammasome activation in rats. *Int J Mol Sci* 2015;16(9):20595–608.
- Zhang H-Y, Wang Z-G, Wu F-Z, et al. Regulation of autophagy and ubiquitinated protein accumulation by bFGF promotes functional recovery and neural protection in a rat model of spinal cord injury. *Mol Neurobiol* 2013;48(3):452–64.
- Sugawara T, Lewén A, Gasche Y, Yu F, Chan PH. Overexpression of SOD1 protects vulnerable motor neurons after spinal cord injury by attenuating mitochondrial cytochrome c release. *FASEB J* 2002;16(14):1997–9.
- Takafumi M, Masaaki T, Satoshi Y, et al. Simulated microgravity facilitates cell migration and neuroprotection after bone marrow stromal cell transplantation in spinal cord injury. *Stem Cell Res Ther* 2013;4(2):35.
- Piantadosi CA. Carbon monoxide, reactive oxygen signaling, and oxidative stress. *Free Radic Biol Med* 2008;45(5):562–9.
- Geralds M, Hendrikj V, Jamesf MLB, Kanji N. Measurement of endogenous carbon monoxide formation in biological systems. *Antioxid Redox Signal* 2002;4(2):271–7.

- [41] Li J, Wang Q, Wang H, et al. Lentivirus mediating FGF13 enhances axon regeneration after spinal cord injury by stabilizing microtubule and improving mitochondrial function. *J Neurotrauma* Feb 2018;1;35(3):548–59.
- [42] Deng J, Lei C, Chen Y, et al. Neuroprotective gases – fantasy or reality for clinical use? *Prog Neurobiol* 2014;115(2):210–45.
- [43] Wu X, Zhang H, Qi W, et al. Nicotine promotes atherosclerosis via ROS-NLRP3-mediated endothelial cell pyroptosis. *Cell Death Dis* 2018;9(2):171.
- [44] Zhang Y, Liu X, Bai X, et al. Melatonin prevents endothelial cell pyroptosis via regulation of long noncoding RNA MEG3/miR-223/NLRP3 axis. *J Pineal Res* 2018;64(2).
- [45] Shi J, Gao W, Shao F. Pyroptosis: gasdermin-mediated programmed necrotic cell death. *Trends Biochem Sci* 2017;42(4):245–54.
- [46] Queiroga CS, Vercelli A, Vieira HL. Carbon monoxide and the CNS: challenges and achievements. *Br J Pharmacol* 2015;172(6):1533.
- [47] Peers C, Boyle JP, Scragg JL, et al. Diverse mechanisms underlying the regulation of ion channels by carbon monoxide. *Br J Pharmacol* 2015;172(6):1546–56.
- [48] Wilkinson WJ, Kemp PJ. Carbon monoxide: an emerging regulator of ion channels. *J Physiol* 2011;589(13):3055–62.
- [49] Zheng M, Zhang Q, Joe Y, et al. Carbon monoxide-releasing molecules reverse leptin resistance induced by endoplasmic reticulum stress. *Am J Physiol Endocrinol Metab* 2013;304(7) (E780–E8).
- [50] Chung J, Shin DY, Zheng M, et al. Carbon monoxide, a reaction product of heme oxygenase-1, suppresses the expression of C-reactive protein by endoplasmic reticulum stress through modulation of the unfolded protein response. *Mol Immunol* 2011;48(15–16):1793–9.
- [51] Ye LB, Yu XC, Xia QH, et al. Regulation of caveolin-1 and junction proteins by bFGF contributes to the integrity of blood–spinal cord barrier and functional recovery. *Neurotherapeutics* 2016;13(4):844–58.
- [52] Gozzelino R, Jeney V, Soares MP. Mechanisms of cell protection by heme oxygenase-1. *Annu Rev Pharmacol Toxicol* 2010;50(1):323–54.
- [53] Grochot-Przeczek A, Dulak J, Jozkowicz A. Haem oxygenase-1: non-canonical roles in physiology and pathology. *Clin Sci* 2012;122(3):93–103.
- [54] Mortezaee K, Khanlarkhani N, Beyer C, Zendedel A. Inflammasome: its role in traumatic brain and spinal cord injury. *J Cell Physiol* 2018;233(7).
- [55] Shi J, Zhao Y, Wang Y, et al. Inflammatory caspases are innate immune receptors for intracellular LPS. *Nature* 2014;514(7521):187–92.
- [56] Kayagaki N, Stowe IB, Lee BL, et al. Caspase-1 cleaves gasdermin D for non-canonical inflammasome signalling. *Nature* 2015;526(7575):666–71.
- [57] Hanamsagar R, Hanke ML, Kielian T. Toll-like receptor (TLR) and inflammasome actions in the central nervous system. *Trends Immunol* 2012;33(7):333–42.
- [58] Pedra JHF, Cassel SL, Sutterwala FS. Sensing pathogens and danger signals by the inflammasome. *Curr Opin Immunol* 2009;21(1):10–6.
- [59] Alnemri ES. Sensing cytoplasmic danger signals by the inflammasome. *J Clin Immunol* 2010;30(4):512–9.
- [60] Vaccari JPDR, Dietrich WD, Keane RW. Therapeutics targeting the inflammasome after central nervous system injury. *Transl Res* 2016;167(1):35–45.
- [61] Wilkinson WJ, Hanne G, Harrison AWJ, Allen ND, Riccardi D, Kemp PJ. Carbon monoxide is a rapid modulator of recombinant and native P2X2 ligand-gated ion channels [Abstract]. *Purinergic Signal* Oct 2009;158(3):862–71.
- [62] Misawa T, Takahama M, Kozaki T, et al. Microtubule-driven spatial arrangement of mitochondria promotes activation of the NLRP3 inflammasome. *Nat Immunol* 2013;14(5):454.
- [63] Han Y, Xu X, Tang C, et al. Reactive oxygen species promote tubular injury in diabetic nephropathy: the role of the mitochondrial ROS-TXNIP-NLRP3 biological axis. *Redox Biol* 2018;16:32.
- [64] Zhou R, Yazdi AS, Menu P, Tschopp J. A role for mitochondria in NLRP3 inflammasome activation. *Nature* 2011;469(7329):221.
- [65] Tufanli O, Telkoparan Akillilar P, Acosta-Alvear D, et al. Targeting IRE1 with small molecules counteracts progression of atherosclerosis. *Proc Natl Acad Sci U S A* 2017;114(8) (E1395–E404).
- [66] Chen D, Dixon BJ, Doycheva DM, et al. IRE1 α inhibition decreased TXNIP/NLRP3 inflammasome activation through miR-17-5p after neonatal hypoxic–ischemic brain injury in rats. *J Neuroinflammation* 2018;15(1):32.
- [67] Joe Y, Kim S, Kim HJ, et al. FGF21 induced by carbon monoxide mediates metabolic homeostasis via the PERK/ATF4 pathway. *FASEB J* 2018;32(5):2630–43.
- [68] Jeong KH, Joe Y, Kim SK, et al. Carbon monoxide protects against hepatic steatosis in mice by inducing Sestrin-2 via the PERK-eIF2 α -ATF4 pathway. *Free Radic Biol Med* 2017;110:81–91.